AD-A262 673

REPORT DOCUMENTATION PAGE

than is estimated to average 1 hour per response, including the time for reviewing instructions, searching existing data sources, gathering and reviewing the collection of information. Send comments regarding this burden estimate or any other aspect of this gathering this burden, to Washington Headquarters Services, Directorate for Information Operations and Reports, 1215 Jefferson 2, and to the Office of Management and Budget, Paperwork Reduction Project (0704-0188), Washington, DC 20503.

2. REPORT DATE	3. REPORT TYPE AND DATES COVERED
2/14/93	2/15/92 - 2/15/93 *Annual*

4. TITLE AND SUBTITLE	5. FUNDING NUMBERS
MULTIPARAMETER RADAR AND AIRCRAFT BASED STUDIES OF THE MICRO-PHYSICAL, KINEMATIC & ELECTRICAL STRUCTURE OF CONVECTIVE CLOUDS	G AFOSR-91-0141 PR 2310 TA CS PE 61102F

6. AUTHOR(S)

V.N. Bringi, I.J. Caylor

7. PERFORMING ORGANIZATION NAME(S) AND ADDRESS(ES)	8. PERFORMING ORGANIZATION REPORT NUMBER
V. N. Bringi/I.J. Caylor Colorado State University Fort Collins, CO 80523 AFOSR-TR- 93 8	

9. SPONSORING/MONITORING AGENCY NAME(S) AND ADDRESS(ES)	10. SPONSORING/MONITORING AGENCY REPORT NUMBER
AFOSR/NL Building 410, Bolling AFB D.C. 20332-6448 Lt Col James Stobie	

DTIC
ELECTE
S APR 0 9 1993
B

11. SUPPLEMENTARY NOTES

12a. DISTRIBUTION/AVAILABILITY STATEMENT	12b. DISTRIBUTION CODE
Approved for Public Release, Distribution is unlimited.	

13. ABSTRACT (Maximum 200 words)

Ongoing studies of the microphysical, kinematic and electrical evolution of two convective clouds observed by radar and aircraft during the Convective and Precipitation Electrification Project (CaPE) are reported. A complete life-cycle of cloud evolution from radar first echo to mature phase is documented using reflectivity (Z_H) and differential reflectivity (Z_{DR}). Aircraft data from T-28, NOAA-P3, NCAR King Air and Wyoming King Air are in the process of being analyzed for particle type, electric field from field mills and up/down draft. Surface field mills and LLP data give an indication of first cloud-to-ground lightning time and location.

Another on-going study is related to multiparameter radar studies of lightning echoes and a triggered lightning event.

466 434

93 4 08 077

93-07444

14. SUBJECT TERMS		15. NUMBER OF PAGES
Radar, electrical, storms, lightning		16. PRICE CODE

17. SECURITY CLASSIFICATION OF REPORT	18. SECURITY CLASSIFICATION OF THIS PAGE	19. SECURITY CLASSIFICATION OF ABSTRACT	20. LIMITATION OF ABSTRACT
Unclassified	Unclassified	Unclassified	UL

NSN 7540-01-280-5500

Standard Form 298 (Rev. 2-89)

1 9 FEB 1993

February 12, 1993

Lt. Col. James Stobie
Program Manager
Directorate of Chemical and
  Atmospheric Sciences
AFOSR, Bldg 410
Bolling AFB, D.C. 20332-6448

Ref: AFOSR-91-0141

Dear Dr. Stobie:

Attached are 6 copies of the second interim report for the above referenced grant. Substantial progress has occurred during the last year in analyzing the CaPE dataset as you can see by the number of papers prepared for the Radar Conference to be held in May in Norman. I have established a useful collaboration with Dr. Andy Detwiler of South Dakota School of Mines and Technology on aircraft data analysis specifically related to T-28 and NOAA P-3. The 9 August CaPE case is the only one with multiple aircraft penetrations of growing convective clouds. The first cloud was captured by radar from first echo, and later penetrated during the growth stage by both NCAR and Wyoming King Airs (KA) as well as the NOAA-P3. The T-28 made two penetrations during the mature phase. It is the best documented case from an aircraft viewpoint. Right now I'm trying to reconcile navigation data from the two KAs. The NOAA P-3 and T-28 navigation were determined to be excellent. The paper by Bringi, Caylor, Turk and Lin documents the analysis so far.

The second cloud of 9 August was also captured from first echo but the initial growth phase was quite different microphysically from the first cloud. The aircraft involved were the T-28 and P-3 but the temporal sampling was not as good as the first cloud. The paper by Bringi, Detwiler et al. documents the analysis so far.

Dr. I. J. Caylor is pursuing analysis of multiparameter radar signatures of 24 natural and one triggered lightning event and is reported in Caylor et. al.

The full list of papers supported by AFOSR and to be presented at the Norman Radar Conference is given below;

1.   Bringi, V. N., A. Detwiler, V. Chandrasekar, P. L. Smith, L. Liu, I. J. Caylor and D. Musil, "Multiparameter radar and aircraft study of the transition from early to mature storm during CaPE: The case of 9 August 1991".

2.   Bringi, V. N., I. J. Caylor, J. Turk and L. Liu, "Microphysical and electrical evolution of a convective storm using multiparameter radar and aircraft data during CaPE".

3.   Caylor, I. J., V. Chandrasekar, V. N. Bringi and S. S. Minger, "Multiparameter radar observations of lightning".

4.   Liu, L., V. N. Bringi, I. J. Caylor and V. Chandrasekar, "Intercomparison of multiparameter radar signatures from Florida storms".

The personnel supported by this grant are Dr. V. N. Bringi, P.I., Dr. I. J. Caylor, Research Associate and Ms. Li Liu, Ph.D. student.

If you should need further information please call me. As this is the final year of the grant, and because of the painstaking data analysis required to combine microphysical, kinematic and electrical measurements into a coherent picture of cloud electrification, I will submit a renewal proposal to AFOSR later this summer. In this regard, any advice from you as to the appropriate submission time would be greatly appreciated.

Sincerely,

V·N·Bringi

V. N. Bringi
Professor
Electrical Engineering

VNB/br

Accession For	
NTIS GRA&I	☑
DTIC TAB	☐
Unannounced	☐
Justification	
By	
Distribution/	
Availability Codes	
Dist	Avail and/or Special
A-1	

MULTIPARAMETER RADAR AND AIRCRAFT STUDY OF THE TRANSITION FROM EARLY TO MATURE STORM DURING CaPE: THE CASE OF 9 AUGUST 1991

V.N. Bringi, A. Detwiler*, V. Chandrasekar, P.L. Smith*, L. Liu, I.J. Caylor and D. Musil*

Colorado State University, Fort Collins, CO

* South Dakota School of Mines and Technology, Rapid City, SD

1.   INTRODUCTION

On 9 August, 1991, convection began forming over the Cape Canaveral area at 16:30 UTC due to interactions between horizontal convective rolls and river breezes. Surface winds were from the W/NW near the Cape area. The 15:00 sounding at Cape Canaveral indicated light westerly winds up to 6 km which then shifted to E/SE winds above 7.5 km. The $0°C$ level was at 4.6 km, and cloud base was at 1.2 km. A cloud which developed over the NASA field mill network was subsequently penetrated by the T-28 at an altitude of 4.8 km msl. The CP-2 radar captured the full cloud evolution from first echo through the mature stage. The cloud was first detected (8.5 dBZ at 4.3 km height, range=23.5 km) at 18:21 UTC (henceforth all times are UTC and all heights are msl). For a few minutes the dual-frequency (S/X-band) reflectivity ratio, DFR, was 8 - 9 dB giving evidence of partial Bragg scattering, the Z_{dr} being 0 dB. At 18:25, Z_h increased to 10 dBZ, the DFR decreased to 0 dB while Z_{dr} jumped to 1.7 dB at 5 km height. This, we believe, is strong evidence for raindrop formation by the warm rain process. At 18.28 a few big drops ($Z_{dr} \sim 3$ - 4 dB) were detected falling to the ground while an anvil from a mature storm (about 10 km to the SE) extended over the cloud of interest at 9 km height. It appears from the radar data that ice crystals from the anvil descended into the upper part of this cloud, freezing it. Z_{dr} was nearly 0 dB above 5.5 km, with large drops continuing to fall out from the cloud. The reflectivity aloft (6 km) intensified to 48 dBZ at 18:36 with Z_{dr} being 0 dB, indicating graupel formation. We refer to this cloud as cell A, to distinguish it from new growth that occurred on the NW side of cell A, a region with persistent updraft. The first evidence of new growth was at 18:35 and this cloud will be called cell B as its evolution could be separately tracked. Its microphysical evolution was rapid and very different from cell A and was responsible, we believe, for cloud electrification which started at 18:41 with the first CG strike at 18:43.

2.   CLOUD EVOLUTION

Fig.1 shows CAPPIs at 5.5 km height with T-28 tracks which penetrated the cloud at 18:36 and 18:41 overlaid. The grey scales depict Z_{dr}, the darker shades representing larger values. Fig.1a shows cell A about 12 min after first echo. Fig.1b shows a positive Z_{dr} column (cell B) while cell A has glaciated (~ 0 dB Z_{dr}). Fig.2 shows vertical sections taken along the shear direction (SE-NW);
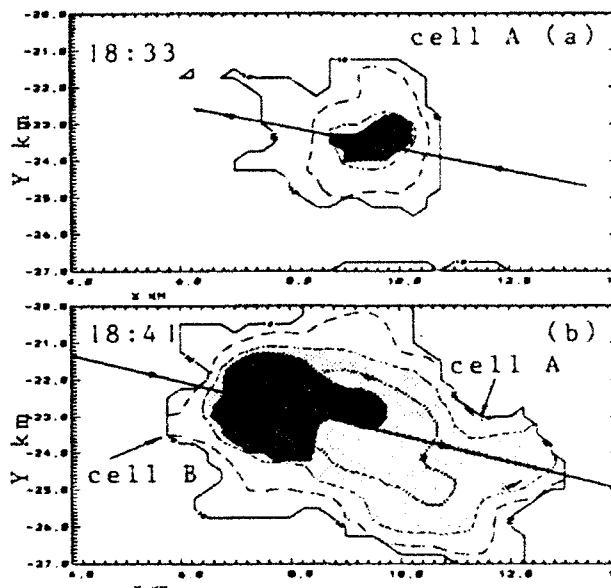

Fig.1 CAPPI at 5.5 km height of Z_h contours (start from 10 dBZ, step 10 dB) with Z_{dr} grey scales (the intervals being 0.5,1.5,3,4 dB).
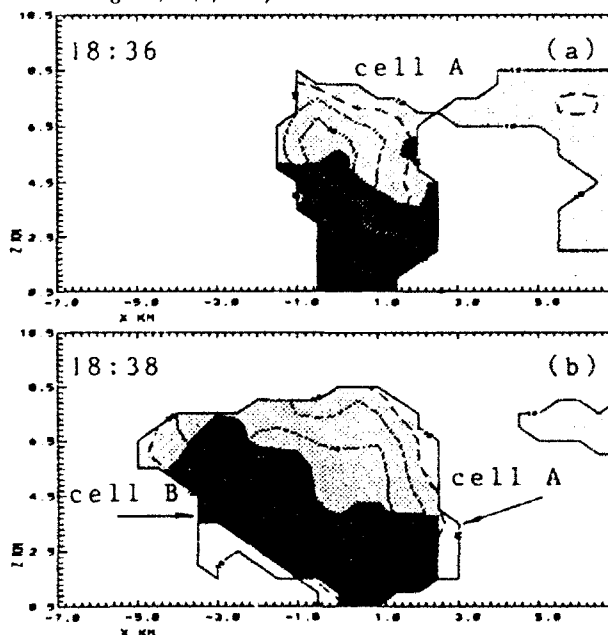

Fig.2 Vertical sections along an SE-NW line in Fig.1. X=0 here is the center of the reflectivity core in Fig.1. Z_{dr} grey scales same as in Fig.1.

positive (negative) X values represent locations SE (NW) of the main echo. Note the positive Z_{dr} column in Fig.2b (cell B). The height profile of Z_{dr} represents updraft conditions in cell B and downdraft in cell A. Fig.3 summarizes T-28 data for the 18:36 (solid lines) and 18:41 (dashed lines) penetrations, which were respectively along the $SE \rightarrow NW$ and $NW \rightarrow SE$ directions. At 18:36 the T-28 detected a peak downdraft of 9 m/s just below the main echo in Fig.2a (cell A). The PMS 2D-P probe as well as the Cannon camera showed a mixture of very wet graupel and drops in the downdraft with maximum sizes of 6 - 7 mm as shown in Fig.3. The LDR was about -23 dB in the downdraft, consistent with wet graupel. A peak updraft of 13 m/s (LWC $\sim$ 1.5 g/m^3) was detected about 2.5 km NW of the main echo in Fig.1a. This was well correlated with the first radar detection of cell B at 18:36 at 5 km height. The T-28 pilot reported moderate rain early during penetration of the updraft. Neither the P-probe nor the Cannon camera detected any drops in the updraft; however, the foil impactor registered a few circular impressions (drops) of 1-2 mm diameter in the updraft. On the return penetration at 18:41, the T-28 sampled cell B (updraft peak $\sim$ 15 m/s, LWC $\sim$ 2 g/m^3) and cell A (downdraft peak $\sim$ 7 m/s, wet graupel 6 - 7 mm). Within the updraft (positive Z_{dr} column, Fig.2b), the P-probe detected a few large drops (5 - 6 mm) while the foil impactor registered eight circular impressions, the largest being 2.5 mm, and about 10s later a large drop ($\sim$ 6 mm). The T-28 pilot reported moderate rain in the updraft. These data are consistent with the positive Z_{dr} column in Fig.2b (cell B) consisting of a low concentration of large drops. The pilot also reported lightning during this penetration as well as a transition from rain to ice on the windscreen as he left the updraft. A dry/wet growth modeling calculation showed that the larger graupel (6 - 7 mm) could be in wet growth. Peak LDR and X-band specific attenuation values of -18 dB and 1 dB/km were observed at the T-28 flight altitude in the downdraft, which are also consistent with wet graupel.

Fig.4a shows the time-height reflectivity profile of cell A starting at 18:23; contours start at 0 dBZ and increment by 5 dB. The dark solid line shows the maximum height reached by the 2 dB Z_{dr} contour. Note the overlying anvil from a mature storm about 10 km to the SE referred to earlier. The arrows represent peak vertical winds from the T-28 penetrations at 18:36, 18:41 and 18:48 and one penetration of the NOAA P-3 at 18:45. The top panel shows the vertical electric field from a surface field mill located under the cloud at X=13, Y=-24 km (see Fig.1b). The dark vertical bars are the maximum vertical component of the E-field from the T-28 field mills. Horizontal dark bars represent the duration of the penetration. The solid triangle at 1200s is the time of the first cloud-to-ground lightning detected by the NASA LLP network (18:43:27 at X=13.5, Y=-24.6 km). Before 600s the surface field mill activity is due to a strong storm located 10 km W/SW. Fields with fair weather polarity start at 700s with a reversal evident at 900s. At 1050s (18:41 T-28 penetration in Fig.3) the electric fields build up at the T-28 altitude
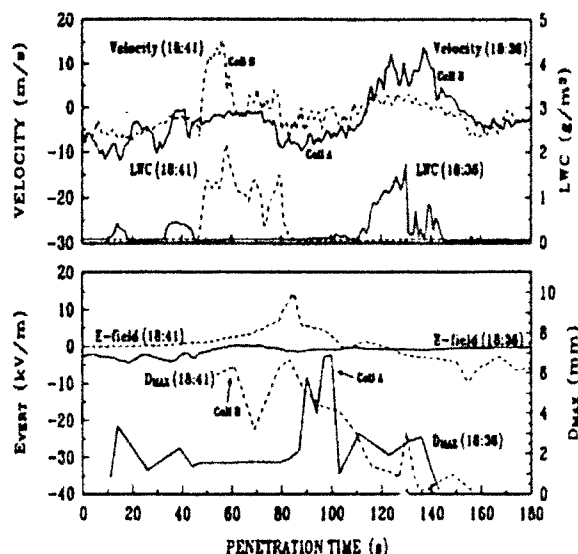

Fig.3 Data from T-28 showing up/downdraft (velocity), liquid water content (LWC), vertical E-field and maximum partical size. The time t=0 is the starting time for each penetration.

with the CG strike following at 1200s. As noted, the T-28 pilot reported lightning during the 18:41 penetration, the surface field mill shows numerous strikes after this time. Cell A shows a general sinking of the reflectivity with time after 700s ($\sim$ 18:34) with some indication of pulsation. The maximum height of the 2 dB Z_{dr} contour also sinks slowly, correlating well with the persistent downdraft measured by the two aircraft.

The evolution of cell B in Fig.4b is quite different. It was first detected as new growth at 700s. The strong updraft detected by the T-28 (Fig.3) correlates well with the positive Z_{dr} column, the 2 dB Z_{dr} height rising to 6 km ($-8°C$). Subsequently, following what appears to be freezing of the raindrops the Z_{dr} height falls while the cloud top grows substantially, possibly due to the associated latent heat release. By the time of the T-28's 18:41 penetration, the 50 dBZ core is at 6.5 km. This was also a region of wet growth as predicted by the growth model. The 2 dB Z_{dr} height doesn't decrease, remaining near the $-3°C$ level indicating persistent updraft as corroborated by the P-3 and T-28 penetrations at 18:45 (1350s) and 18:48 (1500s), respectively. The surface field mill located near cell B at X=7, Y=-22 km (see Fig.1) shows fair weather polarity until 1050s ($\sim$ 18:40), with subsequent electrification until the CG strikes are indicated (top panel). The T-28 and mills also show electrification at the time. It appears that mixed phase microphysics plus the up/downdraft structure played important roles in electrifying the clouds. Detailed analysis of the aircraft data and other radar signatures such as LDR and A_3 will add important details to the cloud evolution.
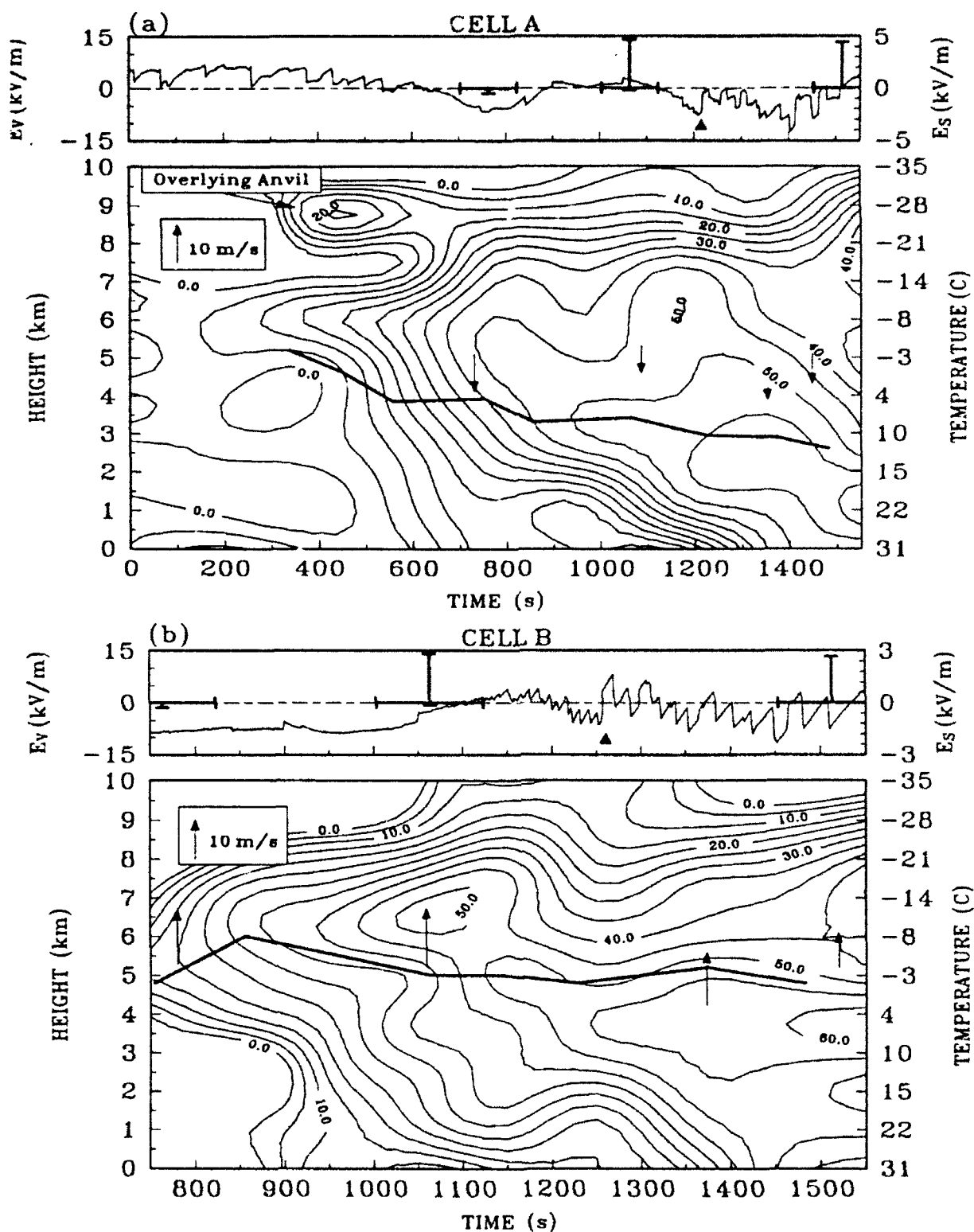
Acknowledgement

Fig.4 Time-height contours of Z_h for cell A (a) and cell B (b). Dark solid line is the maximum height of the 2 dB Z_{dr} level reached at various times. Vertical arrows are peak updraft speeds from T-28 (3) and P-3 (1). Top panels show maximum vertical E-field from T-28, E_v (dark solid bars), and the E-field from surface field mill located near the cells, E_s (light continuous line). The solid triangle mark in (a) at 1210 s, and (b) at 1260 s, is the first CG strike from the cell.

MICROPHYSICAL AND ELECTRICAL EVOLUTION OF A CONVECTIVE STORM USING MULTIPARAMETER RADAR AND AIRCRAFT DATA DURING CaPE

V.N. Bringi, I.J. Caylor, J. Turk and L. Liu

Colorado State University, Fort Collins, CO 80523

1. INTRODUCTION

On 9 August 1991 of the CaPE project the transition from early echo to mature stage was captured by the CP-2 radar as well as two King Airs (NCAR KA and Wyoming KA), the NOAA P-3 and the T-28 aircrafts. It was the only such case in CaPE involving good coordination between the multiple aircraft and radar permitting a study of the microphysical and electrical evolution of the particular cloud. A companion paper by *Bringi* et al. (these Proceedings) deals with the evolution of another adjacent cloud (about 7 km away) which was penetrated by the T-28. The general environmental conditions were quite similar for both clouds and we refer to that paper for details. However, the microphysical evolution has some differences between the two clouds that are interesting.

The cloud was first detected (peak of 3 dBZ at height = 2.6 km and range = 25 km) at 17:48 UTC (henceforth all height are msl and time are UTC). The dual-frequency (S/X-band) reflectivity ratio, DFR, was 15 dB indicating dominance by Bragg scattering. At 17:51, the peak reflectivity increased to 22.5 dBZ, DFR decreased to 0 dB and Z_{dr} increased to 0.75 dB, evidence of coalescence formation of drops. About 10 minutes later (18:00) a strong positive Z_{dr} column had formed, similar to those reported by *Illingworth* (1992) in Alabama during MIST. The warm cloud with a positive Z_{dr} column persisted until 18:09 and then the cloud glaciated, releasing latent heat and accompanied by strong vertical growth. A weak E-field ($\sim$ 5 kV/m) detected by NCAR KA at 18:12 forced it away from the cloud. An enhanced E-field was detected by the NOAA P-3 at 18:16. The first cloud-to-ground lightning from the cloud was detected by the NASA LLP network at 18:18.

2. CLOUD EVOLUTION

Surface winds were from the W/NW near the Cape. The 15:00 sounding at Cape Canaveral indicated light westerly winds up to 6 km turning E/SE above 7.5 km. The $0°C$ level was at 4.6 km, with cloud base near 1.2 km. The LWC observations from aircraft were less than 1 g/m^3 indicating a large amount of mixing in these clouds (adiabatic LWC from sounding was $\sim$ 6 g/m^3).

The cloud (A) of interest was detected (17:55) about 4 km NW of another cloud (B) that was in a more mature phase. Both clouds were about 10 km NE of an intense convective line of thunderstorms. At 18:01, cloud B's reflectivity core ($\sim$ 47 dBZ at 4.5 km) started to descend while the now glaciated upper part of the cloud (4 - 7 km) began to tilt to the NW in response to E/SE winds aloft.
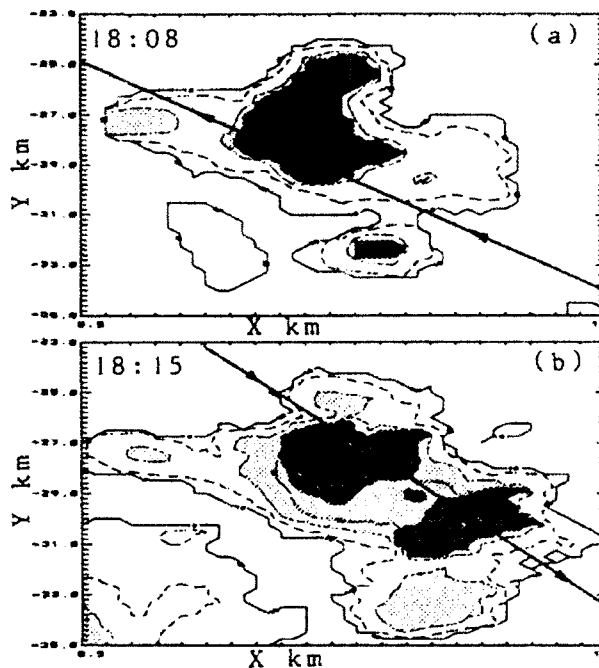

Fig.1 CAPPI at 5.5 km height of Z_h contours with Z_{dr} grey scales. Darker shades are larger Z_{dr}, the intervals being .5,1.5,3,4 dB.

At 18:04, the warm cloud A which was on the up-shear side (top $\sim$ 5 km) had the tilted upper part of cloud B overhead. It is possible that surface outflow from cloud B enhanced low level convergence near cloud A. It is also possible that tiny ice crystals or graupel from cloud B may have descended and melted into cloud A forming tiny drops that can grow quickly to very large raindrops. Indeed at 18:08 the 3 dB Z_{dr} contour in cloud A reached up to 6 km, with maximum Z_{dr} of 4 dB at 4 km height (prior to this the maximum Z_{dr} was 2.5 dB at 3 km, and cloud top was 5 km). Also, cloud B loses its identity after 18:05, more or less merging with cloud A.

Fig.1a,b show CAPPI of cloud A at 5.5 km height at (a) 18:08 and (b) 18:15; contours of Z_h start at 10 dBZ and increment by 10 dB while Z_{dr} is shown as a grey scale with darker shades representing larger Z_{dr}. Cloud A is centered at X=13, Y=-27 km in Fig.1a which also shows the positive Z_{dr} column. In Fig.1b the strength of the column has weakened considerably. The NOAA P-3 penetrations at 18:09 and 18:15 are shown in Fig.1. Figs.2a,b,c show vertical sections taken along a line oriented SE-NW (132° from N) in Fig.1; positive (negative) X represents distance SE (NW) from the core. The positive Z_{dr} column in Fig.2a is clearly visible at 18:08, while at 18:12
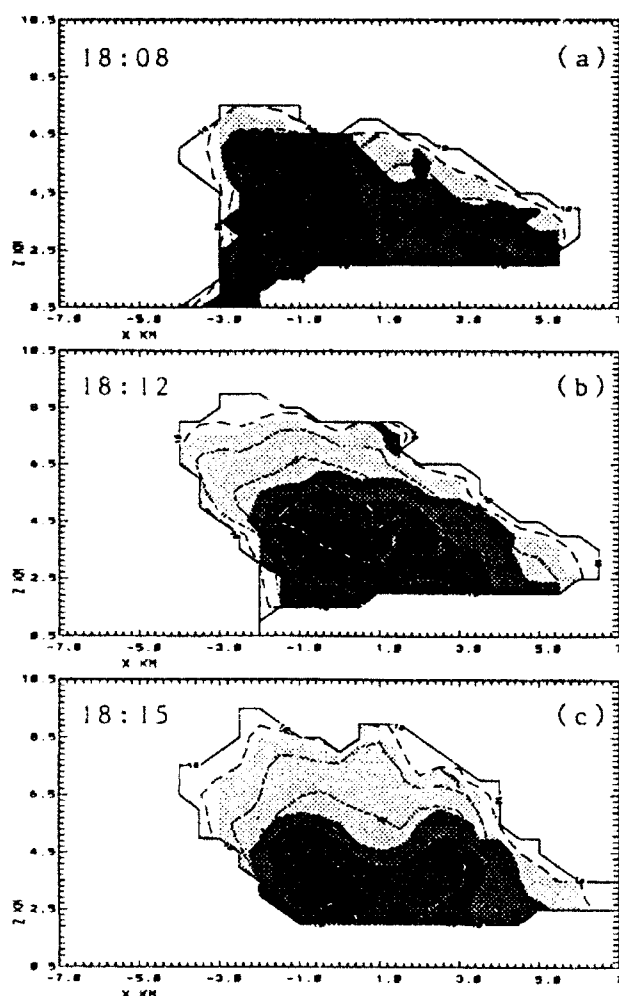
Fig.2 Vertical sections along an SE - NW line in Fig.1. X=0
here is the center of the core in Fig.1. Z_{dr} grey scales
same as in Fig.1.

(Fig.2b) the cloud has glaciated. At 18:15 the reflectivity core was descending and the Z_{dr} structure conforms to the more usual ice-melting-drops situation.

The NOAA P-3 made its penetrations at an altitude of 6.4 km ($-10°C$). Fig.3 shows some of the aircraft measured data during the 18:09 (solid line) and 18:15 (dashed line) penetrations. The top panel shows up/downdraft and liquid water content (LWC), while the bottom panel shows the vertical E-field. At 18:09 the P-3 (going $SE \to NW$) was flying on top of the positive Z_{dr} column (shown in Fig.2a). The main precipitation core ($Z_h \sim 50$ dBZ) was located about 1 km below the flight altitude. Peak Z_{dr} (~ 3 dB) was located at 4.4 km. The updraft location coincides well with the positive Z_{dr} column. Before encountering the updraft (from the SE side of core) the 2D-C probe showed rough edged graupel (maximum dimension ~ 2 mm). Upon entering the updraft, the images were very smooth with particle types being drops and wet graupel. A 3 mm raindrop was detected in the center of the second updraft peak ($\sim 70s$ from 0 in Fig.3). Within the updraft region a high LDR layer was detec...

with values around -17 dB with X-band specific attenuation (A_3) of 1 dB/km. Z_{dr} was around 1 - 1.5 dB. The large LDR signature indicates wet graupel while both Z_{dr} and A_3 are indicative of supercooled drops consistent with the 2D-C images. The E-field is very weak at 18:09.

The NCAR and Wyoming King Air (NKA, WKA) each made a $NW \to SE$ penetration (-3°C, 2.3°C) centered at 18:11. At this time (Fig.2b) the cloud glaciated with cloud top rising from 7.5 km (at 18:08) to 9.0 km (at 18:12). The NKA's penetration at 5.5 km went just on top of the column while the WKA was in the high Z_{dr} region (3 - 3.5 dB) at 4 km height (Fig.2b). The NKA detected a peak updraft of 8 m/s on top of the column and downdraft peak of -3 m/s adjacent to it. At this flight level, a layer of high LDR (-18 to -20 dB) and A_3 (1 - 1.5 dB/km) was noted at the up/down transition. The NKA detected fields of 5 - 6 kV/m and soon exited the cloud. The WKA at lower altitude (4 km) detected a peak updraft of 9 m/s followed by a peak downdraft of -4 m/s separated by 900 m. Large drops (5 - 7 mm) were detected by the P-probe during this penetration.

The P-3 made its reverse penetration (going $NW \to SE$) at 18:15 with data shown in Fig.3. The vertical velocity has decreased substantially and the E-fields have increased dramatically. Fig.2c shows the vertical Z_{dr} structure. At the P-3 flight level (6.4 km), Z_{dr} is nearly 0 dB while LDR is -26 dB and A_3 is near zero. The storm is in its mature phase and the main precipitation core (Z_h peak of 57 dBZ) is descending to the surface. The 2D-C probe detects a much higher concentration of rough-edged graupel (maximum sizes $\sim 2 - 3$ mm).

Fig.4 shows a time-height cross section of cloud evolution from first echo (17:48:00 is t=0) through a 30 min period. The dark solid line is the maximum height reached by the 2 dB Z_{dr} contour. Note the maximum height of 6 km reached at $\sim 18:08$ (1250s from t=0) following which there is a steady decrease to 2 km. The vertical arrows represent updraft detected by the P-3 (6.5 km), NKA (5.5 km) and T-28 (4.8 km) at various times in the cloud evolution. The updraft magnitude decreases with time are roughly correlated with the maximum height of the 2 dB Z_{dr} contour. The top panel shows the detection of the first cloud-to-ground lightning by the NASA LLP network at 18:18:12 at X=14.1, Y=-29.5 km (see Fig.1b). It appears that mixed phase microphysics plus the up/downdraft structure played important roles in electrifying the cloud. Detailed forthcoming analysis of all the aircraft data with radar LDR and A_3 signatures will add important details to cloud microphysical and electrical evolution. This study can be compared to another cloud evolution described by Bringi et al. (these Proceedings).

References

Bringi et al., 1993: 26th Int. Conf. Radar Meteor.
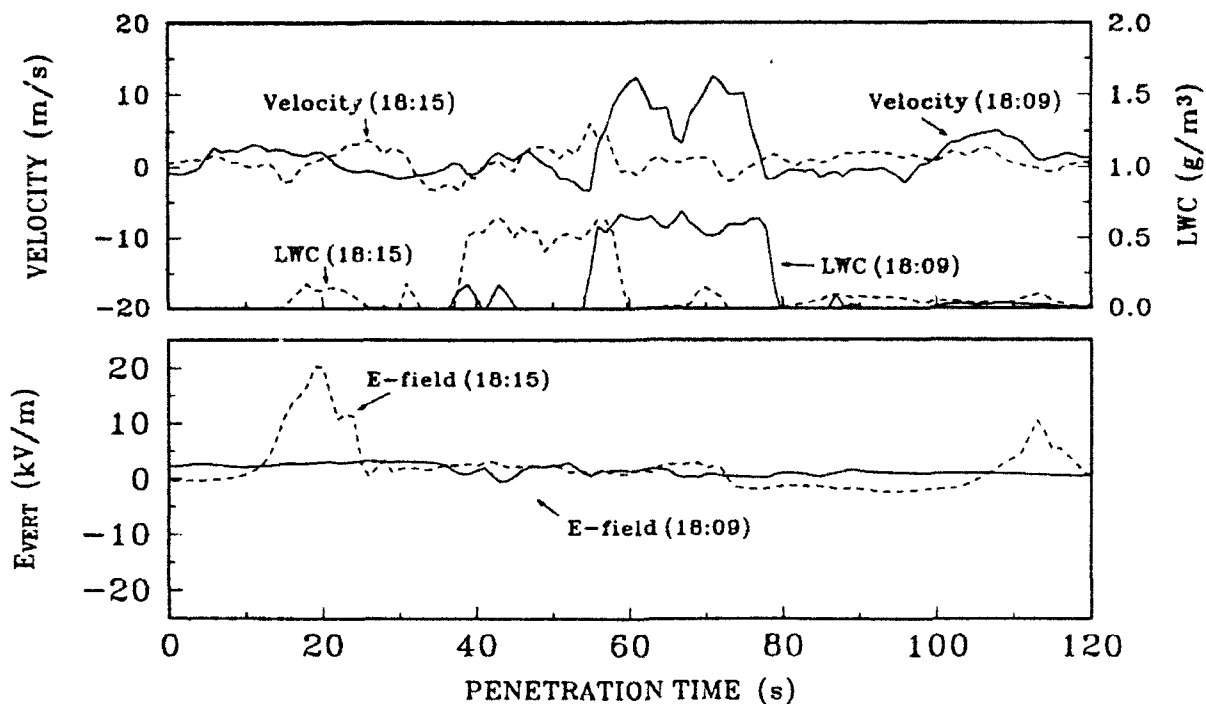Illingworth, 1992: Proc. 11th Int. Conf. Clds. Precip., (1)

Fig.3 Data from NOAA P-3 showing up/downdraft (velocity), liquid water content (LWC) and vertical E-field. The time t=0 is the starting time for each penetration.
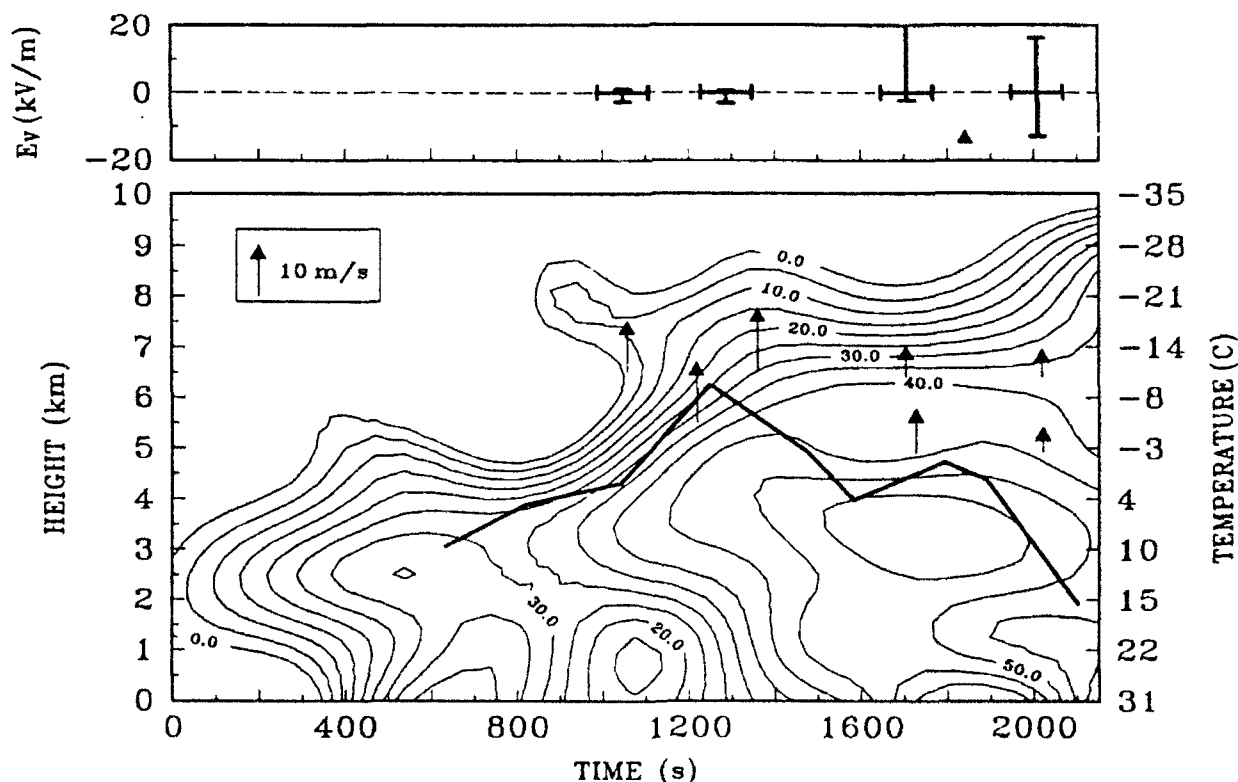

Fig.4 Time-height contours of Z_h. Dark solid line is the maximum height of the 2 dB Z_{dr} level reached at various times. Vertical arrows are updraft speeds from various aircraft. Top panel shows vertical E-field from P-3. The solid triangle mark at 1840s is the first CG strike.

MULTIPARAMETER RADAR OBSERVATIONS OF LIGHTNING

I.J. Caylor, V. Chandrasekar, V.N. Bringi and S.S. Minger

Colorado State University
Fort Collins, CO 80523

1.   INTRODUCTION

Observations of lightning were made in central Florida during the 1991 Convective and Precipitation/ Electrification experiment (CaPE) with the NCAR CP-2 multiparameter radar. Williams et al. (1989) have reported single polarization radar observations of lightning at UHF, S-band, and C-band while more recently Krehbiel et al. (1991) have employed a wideband polarimetric radar at X-band. The CaPE observations presented in this paper are unique in that they were made simultaneously at S- and X-band wavelengths with dual linear polarization.

One of the questions concerning the radar observation of lightning deals with the temperature of the plasma channel. Most recently Holmes et al. (1980) have interpreted their data in terms of a low temperature (underdense) while Williams et al. (1989) have supported the theory of a hot (overdense) plasma. An overdense plasma is a highly conducting target at conventional radar wavelengths and difficulty in detecting lightning at short wavelengths is explained by masking of the lightning by the precipitation echo. The data presented below address this question and the additional polarimetric information provides insight into the spatial geometry of the lightning echo.

2.   OBSERVATIONS

The CP-2 radar operates with a PRF of 960 Hz at a dual wavelength of 3.2 and 10.7 centimeters. The S-band system is coherent and provides estimates of reflectivity (Z_s) and differential reflectivity (Z_{DR}). During CaPE an auxiliary signal processor was implemented on the S-band receiver providing real-time measurements of the differential phase shift (φ_{DP}) between the horizontal and vertical returns and, the correlation coefficient $(|\rho_{HV}(0)|)$ between H and V returns (Chandrasekar et al., 1993). The X-band system provides estimates of the reflectivity (Z_x) and linear depolarization ratio (LDR).

The data described in this paper were collected with the CP-2 radar in a manual mode with the beam stationary in both azimuth and elevation. The X- and S-band antennas have coaxial beams with a width of about 1°.

2.1   Natural lightning

The radar signal processor was configured to integrate data for an interval of 128 pulses (64 horizontal and 64 vertical). The typical range gate spacing was 300 m.

Lightning echoes were observed in thunderstorms above the freezing level at heights between 5 and 12 km and at slant ranges between 35 and 130 km. Figure 1 shows a range profile with a typical lightning echo between 55.5 and 59 km. The lightning is particularly visible as a marked drop in $|\rho_{HV}(0)|$ and an increase of Z_s with a peak excursion of 25 dB above the precipitation echo (58 km). Note the small enhancement of Z_x.
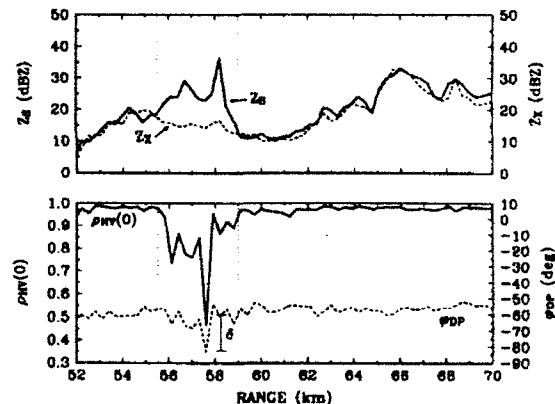

Figure 1. Range profile showing a lightning echo at 55.5 to 59 km. The elevation is 5.58° corresponding to height 5.5 km above ground level.

Range profiles as in Figure 1 were processed to isolate the lightning echo. The profiles were thresholded on an S-band SNR of 30 dB removing weak, noisy signals. The lightning signature was then isolated by flagging points in the profile where Z_s deviated by 2.0 dB and $|\rho_{HV}(0)|$ deviated by 0.075 from their respective means. The mean for each parameter was computed by averaging 10-15 profiles (~1.5 s) prior to the lightning. The flagged lightning echoes were extracted for further analysis.

24 events spread over 6 different days were selected for this paper from the events logged during the CaPE

campaign. It is worth noting that typically the duration for each event spanned two or more integration cycles and extended over several kilometers range. Therefore 155 data points were available for statistic analysis.

Using data extracted from the lightning signatures, the distribution of η (reflectivity in units of cross-section per unit volume) is shown in Figure 2 for X- and S-band. The corresponding distributions Z_{DR}, LDR, and $|\rho_{HV}(0)|$ are shown in Figures 3, 4, and 5.
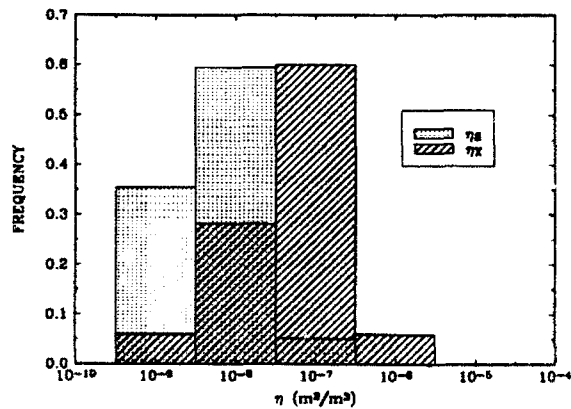

Figure 2. Reflectivity distributions for S-band and X-band. The mean for η_s is 3×10^{-8} m²/m³, while the mean for η_x is 3×10^{-7} m²/m³.
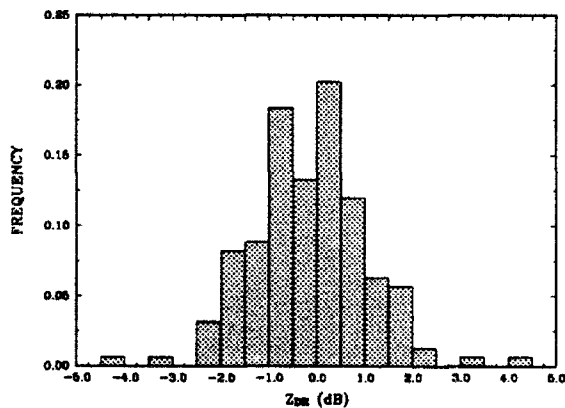

Figure 3. The differential reflectivity distribution with a mean value of -0.2 dB and σ=1.2 dB.

The differential phase shift upon backscatter (δ) was estimated by subtracting φ_{DP} for each lightning echo from the computed mean φ_{DP} profile. A histogram of the estimated δ is shown in Figure 6.

2.2   Triggered lightning

During the CaPE campaign, NASA and French teams engaged in triggered lightning experiments using wire
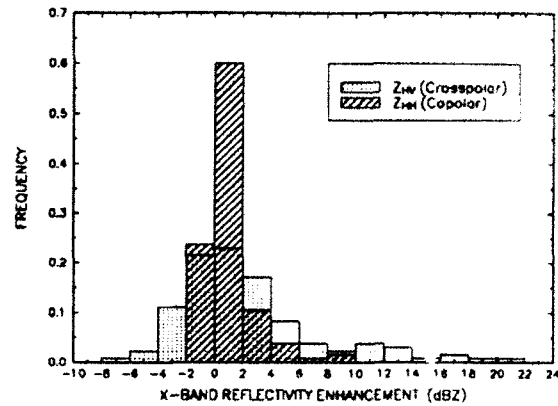

Figure 4. Distributions of the enhancement of the copolar and cross-polar X-band reflectivities due to lightning.
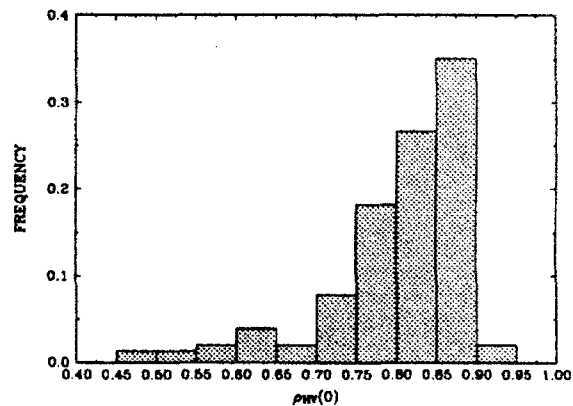

Figure 5. Distribution of the copolar correlation with a mean of 0.8 and σ = 0.086.
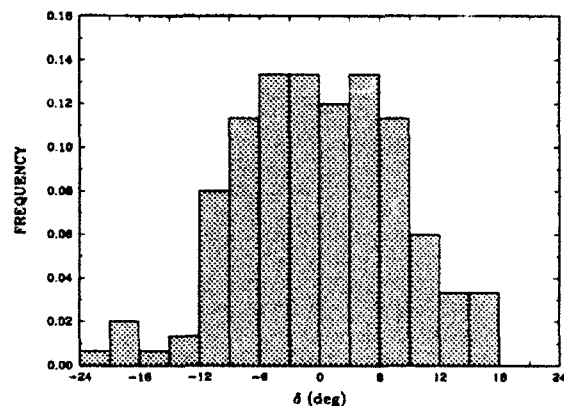

Figure 6. Distribution of backscatter differential phase shift with a mean of 0.7° and σ = 9.5°.

trailing rockets. The land-based launch site was located approximately 7 km to the south east of CP-2. On 25 August 1991, lightning was triggered at 17:50:57.130 GMT at which time the CP-2 antenna was positioned over the launch site at an elevation of 5° (height = 610 m). The RP-6 signal processor was in a time-series collection mode with a range gate spacing of 250 m and an integration interval of 256 pulses.

There was very little precipitation over the launch site at the time of the triggering and so precipitation masking is negligible. The radar echo had a duration of approximately 500 ms, a Z_{DR} of -4 dB, Z_S of 32 dBZ.

3. DISCUSSION

If a power law dependence on wavelength is assumed for lightning reflectivity ($\eta \propto \lambda^n$), the value of n can be computed from simultaneous observations at two wavelengths. For each S- and X-band data pair (Fig. 2) the exponent was computed. The results in Figure 7 show a mean value near -2 and support the λ^{-2} dependence found by Williams et al. (1989) who used UHF, S- and X-band.

The time series for the triggered lightning were analyzed in a similar manner with the exponent being computed for each pair of dual wavelength pulses. Surprisingly the mean value for n is near +1.5 (Fig. 7). A straightforward interpretation of this result is that the channel is underdense. However video photography of the triggered lightning indicates the channel had a large 3 dimensional curvature and so it is possible that the lightning was being observed in the antenna sidelobes. Further analysis of these time series, including a Doppler spectral analysis, along with ground based electrical data is planned.
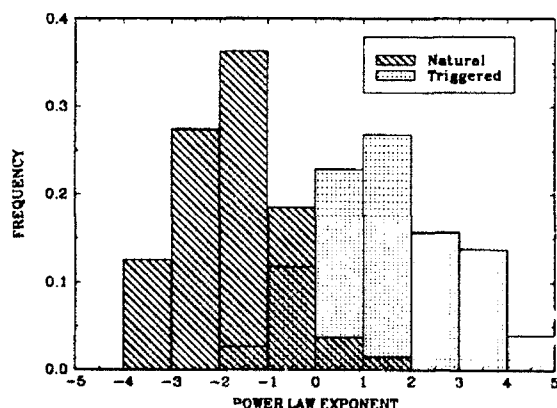

Figure 7. Distribution of the power law exponent, n, for natural (mean of -1.7) and triggered lightning (mean of 1.5).

In general the polarimetric signatures (Figs. 3-6) indicate the lightning target is geometrically complex. The wide variation of Z_{DR} and δ with means near zero indicate no preferred orientation of the target. The 2.4 dBZ enhancement of the X-band crosspolar reflectivity is indicative of a randomly oriented target as well.

Analysis shows that decreases in $|\rho_{HV}(0)|$ are not correlated with large δ. It is possible that the small $|\rho_{HV}(0)|$ and large δ are due to multiple scattering interactions between individual lightning elements within the pulse volume.

4. CONCLUSION

Multiparameter radar observations of natural lightning during the CaPE project show:

• The parameter $|\rho_{HV}(0)|$ decreases dramatically for the lightning echo and coupled with Z_S is an excellent polarimetric signature for lightning.

• There is a λ^{-2} dependence between X-band and S-band reflectivities for lightning in precipitation.

• X-band cross-polar results indicate the lightning echo is depolarizing. Z_{DR} data show that there is no apparent channel orientation. In addition there is a large backscatter differential phase shift of up to ±15° which is uncorrelated with low $|\rho_{HV}(0)|$.

• The only triggered lightning observed during CaPE displays an unusual signature. Further observations of triggered lightning would be of great benefit.

5. REFERENCES

Chandrasekar, V., G.R. Gray, and I.J. Caylor, 1993: Auxiliary signal processing system for a multiparameter radar. *J. Atmos. Ocean. Tech.*, in press.

Holmes, C.R., E.W. Szymanski, S.J. Szymanski, and C.B. Moore, 1980: Radar and acoustic study of lightning. *J. Geophys. Res.*, 85, 7517-7532.

Krehbiel, P.R., W. Rison, S. McCrary, T. Blackman, and M. Brook, 1991: Dual-polarization radar observations of lightning echoes and precipitation alignment at 3 cm wavelength. *Proc. 25th Conf. Radar Meteorology*, Paris, Amer. Meteor. Soc., 901-904.

Williams, E.R, S.G. Geotis, and A.B. Bhattacharya, 1989: A radar study of the plasma and geometry of lightning. *J. Atmos. Sci.*, 46, 1173-1185.

INTERCOMPARISON OF MULTIPARAMETER RADAR SIGNATURES FROM FLORIDA STORMS

L. Liu, V.N. Bringi, I. J. Caylor and V. Chandrasekar

Colorado State University, Fort Collins, CO 80523

1.   INTRODUCTION

The CaPE project offered the first opportunity to collect dual-polarized, dual-frequency radar data in the subtropical regime of central Florida. This paper is based on CP-2 time series data collected at vertical incidence in light rain, and in a squall line case at close range. Each time series record consisted of 128 H and 128 V samples at S-band, and 256 H samples at X-band. From these data, reflectivity at horizontal polarization Z_h, Z_{dr}, copolar correlation coefficient $\rho_{hv}(0)$, differential propagation phase ϕ_{dp} and dual-frequency (S/X) reflectivity ratio DFR were calculated. A new algorithm for calculating specific attenuation A_3 at X-band and specific differential phase K_{dp} is used based on *Hubbert* et al. (1993), which accounts for hail signal and phase shift upon backscatter fluctuations which may be superimposed on the range profiles of DFR and ϕ_{dp}, respectively.

2.   CP-2 RADAR MEASUREMENTS

The radar data reported here were collected on 24 August, 1991 of the CaPE project.

2.1.   Vertically Pointing Data

Raindrops at vertical incidence form a standard target for polarization measurements because of rotational symmetry of the drops when viewed vertically. In addition, if the antenna is rotated a full 360°, the polarization plane also rotates with it. For this method to work the melting level must be located beyond the far-field of the antenna (in this case ~ 1.5 km), a common situation in Florida but not in Colorado, for example.

Fig.1 shows vertical profiles of Z_h, $\rho_{hv}(0)$, ϕ_{dp}, and DFR in light rain at 90° elevation angle. These data have not been filtered in range. The vertical bars in each case show the sample standard deviation. The Z_h brightband is clearly visible at 3.5 km (all heights are agl) The dip in $\rho_{hv}(0)$ to 0.92 at 3.25 km is also clearly noted. Note that $\rho_{hv}(0)$ is estimated from the power time series (see *Liu* et al , these Proceedings). The mean value of $\rho_{hv}(0)$ in light rain below the bright-band is around 0.982. It is well known that $\rho_{hv}(0)$ should be very close to unity in light rain even at horizontal incidence with values of 0.997 quoted by *Illingworth & Caylor* (1991). At vertical incidence the deviation from 1 should be even less. One possible reason for the measured $\rho_{hv}(0)$ being so low is that the phase difference between the HH and VV antenna patterns within the main lobe deviates due to feedhorn imperfections or loss of precision of the reflector shape. Simulations show that this effect is sufficient to drop $\rho_{hv}(0)$ to 0.99 (see *Xiao* et al., these Proceed-
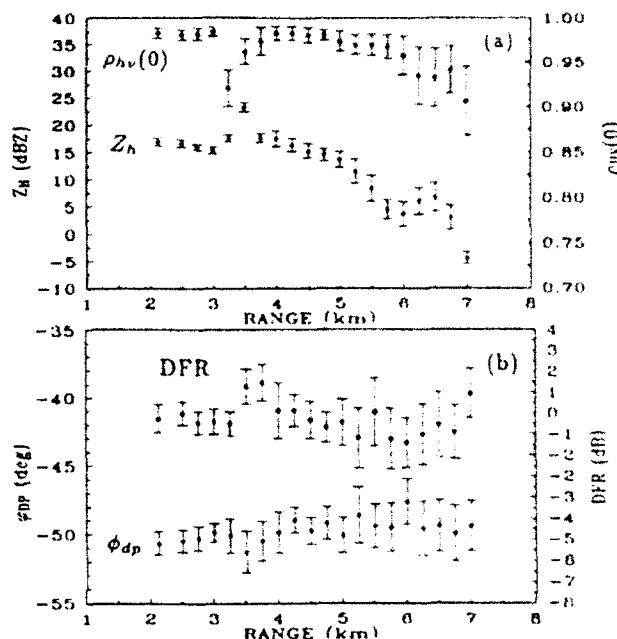

Fig.1 Range profiles of mean and standard deviation of
(a) Z_h, and $\rho_{hv}(0)$,
(b) ϕ_{dp} and DFR from vertical pointing data.

ings). The increase in σ with height > 5.5 km is due to SNR becoming smaller. The large σ at the $\rho_{hv}(0)$ dip is consistent with theory (see *Liu* et al., these Proceedings) and with the results of *Illingworth & Caylor* (1991). The system $\phi_{dp}(\sim -50.5°)$ can be obtained from Fig.1b since at vertical incidence no differential propagation effects are expected in light rain. The DFR results are also shown in Fig.1b. Note the positive fluctuation of about 1.5 dB in the mean at 3.75 km, very close to the peak Z_h. This is suggestive of 'Mie scattering effects due to large, wet snowflakes with maximum size around 10 mm. An assessment of the overall accuracy in derived specific attenuation (A_3, $dB km^{-1}$) and specific differential phase (K_{dp},° km^{-1}) can be made since the mean should equal zero in light rain. Errors may be due to statistical fluctuations, system effects, and the algorithms used to estimate A_3 and K_{dp}. Here we use an adaptation of range filters described by *Hubbert* et al (1993) to calculate A_3 and K_{dp}. The accuracy in estimating the mean value is defined here as the sum of the absolute value of the bias and the 95% confidence interval which is 0.2 - 0.25 ($dB km^{-1}$ or ° km^{-1}) for both A_3 and K_{dp}. Note the condition at vertical incidence, i.e., high SNR, narrow spectrum width and very high $\rho_{hv}(0)$.
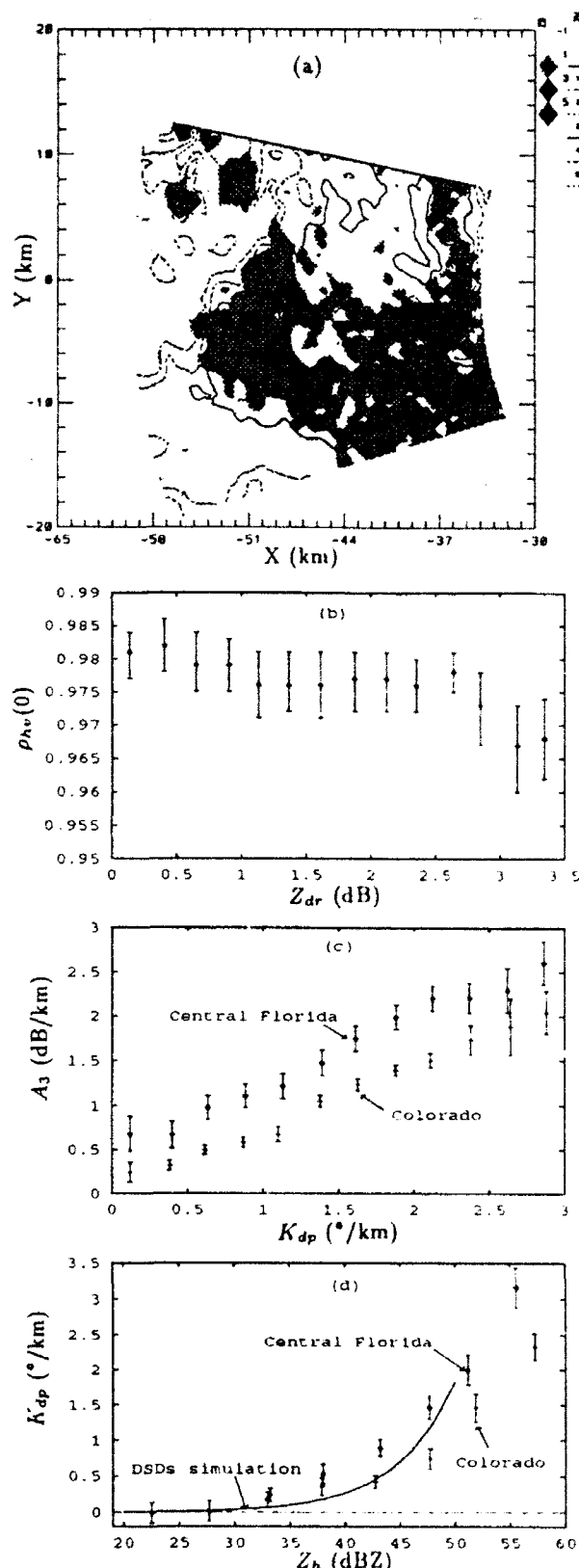
2.2.   Rainfall Data

On 24 August 1991 a squall-line approached the radar from the W-NW. Z_h, Z_{dr}, DFR, φ_{dp} and $\rho_{hv}(0)$ have been filtered in range using an IIR filter which sharply attenuates spatial fluctuations 250 m and less.

Fig.2a shows a PPI scan of Z_h at 1.5° elevation angle derived from the central Florida data. Grey scales correspond to Z_{dr} with darker shades representing higher values.

Fig.2b shows a plot of $\rho_{hv}(0)$ vs Z_{dr} obtained from the 1.5° elevation PPI in Fig.2a between 38 - 48 km. The mean $\rho_{hv}(0)$ does decrease with increasing Z_{dr}, in agreement with theory, but the $\rho_{hv}(0)$ values are significantly lower compared to both theory and the experimental results of *Illingworth & Caylor* (1991). We refer to *Xiao* et al. (these Proceedings) for a further discussion of antenna effects related to the lowered values of $\rho_{hv}(0)$.

Fig.2c shows A_3 vs K_{dp} in rain from data collected at 1.5° elevation (37 - 48 km) and subsequently, at elevation angles 2 - 4° (14 - 26 km). The mean and 95% confidence intervals are shown in Fig.2c and are marked as data from central Florida. Another curve marked 'Colorado' is CP-2 time series data from a rainshaft in a Colorado storm at low elevation angle (1°) at range 82 - 93 km. These data have been processed exactly the same as for the central Florida data. In the K_{dp} range $1 - 2.25° km^{-1}$, the two data sets have different slopes; the central Florida data has a slope of 1.05 while the Colorado data has a slope of 0.78. Also, for a given K_{dp}, the A_3 values in Colorado are consistently less than in central Florida. We believe that these features are statistically significant and are a manifestation of microphysical differences between the two regimes, principally ralated to drop size distributions, and secondarily to mean raindrop shape vs size relations. The Colorado slope of 0.78 is very close to that predicted theoretically by *Bringi* et al. (1990) for Gamma DSDs (0.8), and for experimental DSDs (collected in Norman, OK) from surface distrometer (0.79) assuming equilibrium raindrops shape vs size relation due to *Green* (1975). The results from Fig.2c are independent of absolute system gain and as a consequence are more reliable.

Fig.2d shows the mean K_{dp} vs Z_h for the central Florida and Colorado datasets. The solid line is the mean relationship from simulations using Gamma DSDs. Again, for a given K_{dp}, the Z_h in Colorado is as expected larger than in central Floridais.

2.3. Vertical Cross Sections through A Squall Line

We now show vertical cross sections through the most intense part of the 24 August squall line. Fig.3 shows an RHI scan taken to the west of the radar. Darker shades represent higher values of Z_{dr} and A_3. Contours start at 10 dBz and increament by 10 dBz. These data were collected in the normal operating mode of the CP-2 radar which does not allow for computation of differential phase and $\rho_{hv}(0)$. Fig.3a shows Z_h contours with Z_{dr} grey scales overlayed, while Fig.3b show contours of Z_h with A_3 overlayed. The leading edge of the squall line is at 18 km range. Note the positive Z_{dr} column at 22 km, with the
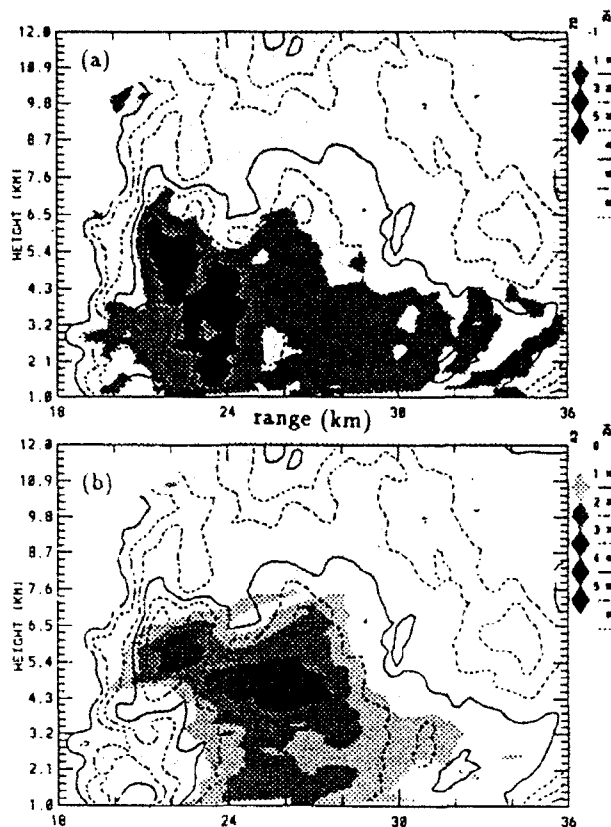
Fig.2 (a) Z_h contours with Z_{dr} grey scales overlayed;
(b) mean and 95% c.i. of $\rho_{hv}(0)$ vs Z_{dr};
(c) mean and 95% c.i. of A_3 vs K_{dp};
(d) mean and 95% c.i. of K_{dp} vs Z_h.

Fig.3 Z_h contours with (a) Z_{dr}, (b) A_3, grey scales overlayed.

Fig.4 Range profiles of (a) Z_h and Z_{dr}; (b) ϕ_{dp} and K_{dp}; (c) Z_h and $\rho_{hv}(0)$; (d) DFR and A_3.

2 dB contour reaching 6.5 km agl. The peak Z_{dr} is 4.5 dB at 5 km agl. The A_3 core is located at 4.5 km agl in Fig.3b in the range sector 24 - 27 km where Z_{dr} is 1.5 - 2.0 dB. This A_3 core represents the main precipitation mass. On the inflow side, a secondary A_3 maximum can be located at 6 km agl in the range 22 - 23 km which also coincides with high Z_h (60 dBZ) and high Z_{dr} (3.5 - 4 dB). This region consists of large raindrops suspended by the updraft.

About 3 minutes later, time series data were collected through the same storm at the same location as described in Fig.3. Range profiles at elevation angle 11° are shown in Fig.4. This profile intersects the main precipitation mass shown in Fig.3b at 4.7 km agl, range = 25 km. Fig.4a,b shows range profiles of Z_h, Z_{dr}, ϕ_{dp} and K_{dp}. Note the peak K_{dp} of $4.75°km^{-1}$ corresponding to a rainfall rate of $150mmh^{-1}$. Note the decrease in Z_{dr} from 3.75 dB at 23.5 km to 0.5 dB at 29 km, indicating the transition from rain to ice. Fig.4c,d show range profiles of Z_h, $\rho_{hv}(0)$, DFR and A_3. From 23 to 29 km, $\rho_{hv}(0)$ (unfiltered in range) decreases from 0.98 to 0.93 indicating a transition from rain to ice. Beyond 30 km, the average $\rho_{hv}(0)$ is 0.96, and beyond 35 km it is 0.985. The peak A_3 is 4.7 $dBkm^{-1}$ and its location coincides with the peak K_{dp} location. The DFR curve decreases with range from 30 km onwards as the X-band signal falls below noise level due to attenuation.

3. CONCLUSIONS
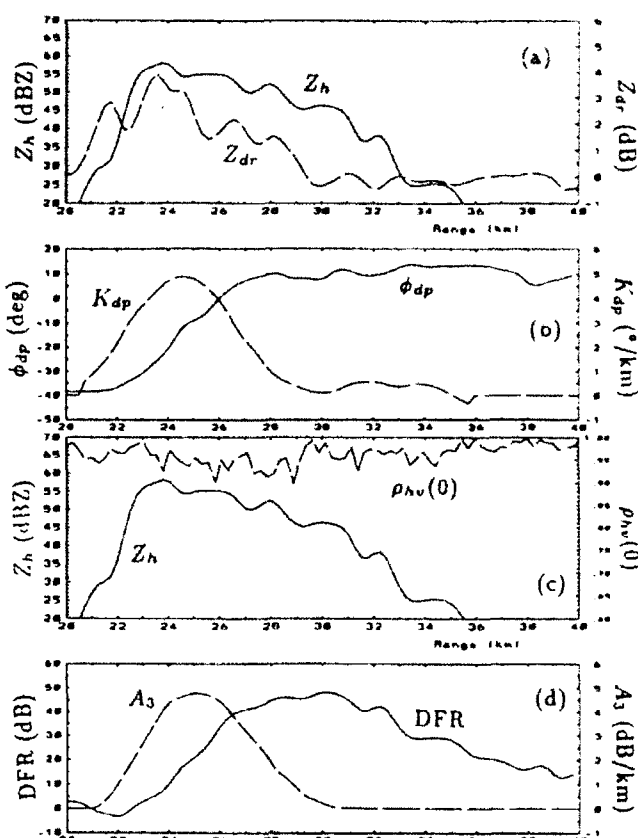
Vertical incidence data in light rain revealed a dip in

$\rho_{hv}(0)$ just below the bright-band, as well as weak Mie scattering effects. The accuracy in estimating A_3 and K_{dp} (from the vertical incidence data) was established to be 0.2 $dBkm^{-1}$ or $°km^{-1}$.

Data from central Florida and Colorado were compared in convective rainfall which showed differences attributable to drop size distribution variations and to a lesser extent variations in the mean raindrop shape vs size relation.

Vertical sections of data through the intense portion of a squall line revealed interesting microphysical features such as a positive Z_{dr} column adjacent to the leading edge, the transition from rain to 'rain + ice' to ice as revealed by $\rho_{hv}(0)$, and the large values of A_3 and K_{dp} within the main precipitation mass.

Acknowledgement

References

Bringi et al., 1990: J. Atmos. Oceanic Tech.
Green et al., 1975: J. Appl. Meteor.,(14)
Bubbert et al., 1993: (to appear) J. Tech.
Illingworth et al., 1991: 25th Conf. Radar Meteor.
Liu et al., 1993: 26th Int. Conf. Radar Meteor.
Xiao et al.,1993: 26th Int. Conf. Radar Meteor.